J Mater Sci (2011) 46:4157–4161
DOI 10.1007/s10853-011-5248-7

IIB 2010

Aberration corrected scanning transmission electron microscopy and electron energy loss spectroscopy studies of epitaxial Fe/MgO/(001)Ge heterostructures

Jaume Gazquez · Maria Varela · Daniela Petti · Matteo Cantoni · Christian Rinaldi · Stefano Brivio · Riccardo Bertacco

Received: 30 August 2010 / Accepted: 6 January 2011 / Published online: 25 January 2011

Abstract Aberration correction in the scanning transmission electron microscope combined with electron energy loss spectroscopy allows simultaneous mapping of the structure, the chemistry and even the electronic properties of materials in one single experiment with spatial resolutions of the order of one Ångström. Here the authors will apply these techniques to the characterization of epitaxial Fe/MgO/(001)Ge and interfaces with possible applications for tunneling junctions, and the authors will show that epitaxial MgO films can be grown on a (001)Ge substrates by molecular beam epitaxy and how it is possible to map the chemistry of interfaces with atomic resolution.

Introduction

Epitaxial growth of insulator oxides on semiconductors constitutes a key issue within the field of electronics, and a considerably large effort has been devoted to harness the growth of high-k oxides on Si. Ge, due to its high electronic and hole mobility, is a very interesting alternative as a potential substrate for future high performance complementary metal–oxide–semiconductor field-effect transistors. However, a major issue is to avoid the high resistivity at the source and drain contacts ensuing from the pinning of the Fermi level at the valence-band maximum. It has been suggested that this problem could be fixed by depositing a thin insulating tunneling barrier between the Ge substrate and the metal contacts [1, 2]. In this case, single crystal epitaxy would represent an additional benefit, since it would lead to a reduction of interfacial defects and improved performance of the tunneling barrier. MgO has been suggested to fulfill such requisites. Furthermore, MgO has been demonstrated to be a good substrate for epitaxial growth of transition metals thin films, such as Fe and Co [3], thus avoiding the potential problem of chemical reactivity with Ge. In such a scenario, epitaxial deposition of high quality MgO films on Ge substrates is highly desirable. But in addition, successful epitaxial growth of MgO on a semiconductor would also constitute a plus for applications in spintronics, since the injection of a spin polarized current from a ferromagnetic electrode to a non-magnetic semiconductor requires the presence of a potential barrier. MgO represents a convenient choice because the symmetry filtering properties at the interface with transition metals would allow an efficient spin filtering effect [4]. For this approach to succeed, a suitable semiconducting substrate where MgO can be grown epitaxially must be found. And again, while GaAs and Si have been investigated for such role, Ge has not received much attention so far [5].

In this study the authors report on the atomic resolution characterization of high quality interfaces in Fe/MgO/(001)Ge heterostructures. The study of the defects, the inhomogeneities and the interface structure of such junctions is a must to pave the way toward future applications. For this aim, the combination of scanning transmission electron microscopy (STEM) and electron energy loss spectroscopy (EELS) is a most useful tool, since it allows

J. Gazquez · M. Varela (✉)
Oak Ridge National Laboratory, Oak Ridge, TN 37830, USA
e-mail: mvarela@ornl.gov
URL: http://stem.ornl.gov

J. Gazquez
Department Física Aplicada III, University Complutense of Madrid, Madrid, Spain

D. Petti · M. Cantoni · C. Rinaldi · S. Brivio · R. Bertacco
Dipartimento di Fisica—Politecnico di Milano, L-NESS, Via Anzani 42, 22100 Como, Italy

these features to be probed with atomic resolution [6–11]. Spherical aberration correction in the STEM allows for increased contrast, allowing even single atoms to be detected both in imaging and spectroscopy [12, 13].

Experimental procedure

The samples used for this study were Fe/MgO/Ge heterostructures grown by molecular beam epitaxy (MBE) on Ge substrates as reported elsewhere [14]. The optimal growth conditions for achieving high quality heterostructures consist in (i) room temperature (RT) growth of MgO followed by post annealing at 500 °C in case of n-doped Ge substrates and (ii) RT growth of Fe followed by annealing at 200 °C. Specimens for STEM observations were prepared by conventional thinning, grinding, dimpling and Ar ion milling. The thin films were observed in a Nion UltraSTEM column, operated at 100 kV, equipped with fifth order Nion aberration corrector and a Gatan Enfina EEL spectrometer.

Results and discussion

Figure 1a shows a low magnification annular dark field (ADF) image of a Fe/MgO/Ge($n = 10^{15}$ cm^{-3}) heterostructure. The MgO and Fe film thicknesses were 3 and 10 nm, respectively. A gold capping layer nominally 3 nm thick was deposited to protect the sample against oxidation, although in some parts of the STEM specimens the Au capping was missing, such as the area in Fig. 1a The layers are continuous over long lateral distances, as also shown in Fig. 2a for a Fe/MgO/Ge($n + 10^{20}$ cm^{-3}) heterostructure. The heterostructure is epitaxial, although the interfaces show some step disorder, Occasionally, steps one unit cell high are observed, giving rise to some roughness. Figure 1b shows a high magnification ADF Z-contrast image of the heterostructure down the [110] Ge projection. The contrast in Z-contrast images is roughly proportional to Z^2 (Z being the atomic number) so heavier atomic columns can be easily distinguished from lighter ones. The thin epitaxial bcc Fe(001) film grows pseudomorphically on a rocksalt MgO(001) substrate with the MgO rotated by 45° with respect to the Fe and Ge lattices, i.e., Fe[100]/MgO[110]/Ge[100] in the interface plane. This rotation produces a misfit strain, which may be released by mismatch dislocations [15]. Indeed, in agreement with previous studies [3], such dislocations are found every few nm for both the Fe/MgO and the MgO/Ge interfaces, as shown in Fig. 2b. The MgO/Ge interface is not perfectly coherent although there is a clearly defined epitaxial relationship between both materials. Regarding the detailed interface

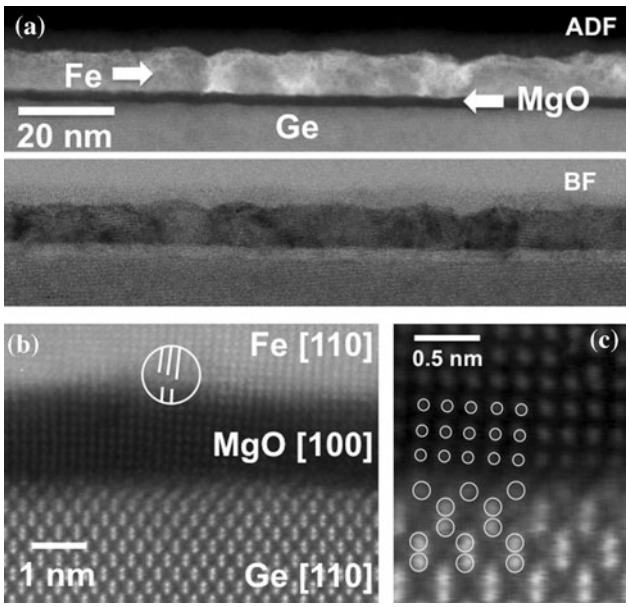

Fig. 1 **a** Low magnification ADF image (*top*) and simultaneous bright field (*bottom*) images of the epitaxial Fe/MgO/Ge(001) heterostructure showing continuous layers over lateral distances of the order of 100 nm. **b** High resolution ADF image of the interfaces, which preserve the orientation relationship but are not fully coherent. A *circle marks* the position of a mismatch dislocation. **c** Magnified image of the Ge–MgO interface, showing a relatively good lattice match. The Ge and the Mg–O columns are marked with *big* and *small circles*, respectively

structure, one cannot tell from these images whether Mg or O are sitting on top of Ge atoms (marked in red on the image), since along this projection the Mg–O columns are a projection including both kinds of atoms. The MgO layers buckle a small angle away from the interface plane, most likely to accommodate steps on the Ge surface.

EELS spectrum images with atomic resolution were acquired in order to probe the compositional sharpness of the Fe/MgO and the MgO/Ge interfaces. Figure 3a shows an atomic resolution ADF image of the Fe/MgO/Ge heterostructure. The Nion UltraSTEM column is ideally suited for EEL spectroscopic imaging at atomic resolution [16]. The box along the interfaces in Fig. 3a shows the spectrum image region, with the simultaneously acquired ADF signal is shown in the bottom panel. Some minor spatial drift in the direction parallel to the interface is observed through the spectrum image. The image is 29 × 100 pixels, and the nominal acquisition time was 0.05 s per pixel. The probe forming aperture had a semiangle of approximately 25 mrad. The collection angle at the spectrometer was estimated to be 34 mrad. EEL spectra in the SI cover an energy range from 400 to 1700 eV, roughly. Such a wide energy range allows simultaneous acquisition of the most important edges of interest for the system: O *K*, Fe $L_{2,3}$, Ge $L_{2,3}$, and Mg $L_{2,3}$, nominally around 530, 708, 1217, and 1305 eV, respectively. Elemental mapping is then possible

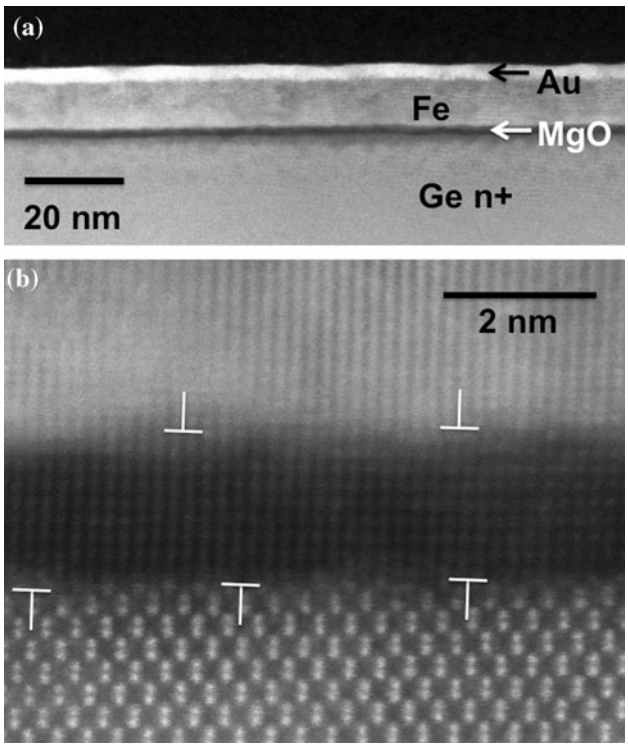

Fig. 2 ADF images of a Fe/MgO/Ge(001) heterostructure grown on a n^+ (10^{20} cm^{-3}) doped Ge substrate. **a** Low magnification image showing flat layers, continuous over long lateral distances. The different layers (Au, Fe, MgO, and the Ge substrate) are labeled on the image. **b** High resolution ADF image. The mismatch dislocations, spaced a few nm, are marked on both the Ge–MgO and the MgO–Fe interfaces

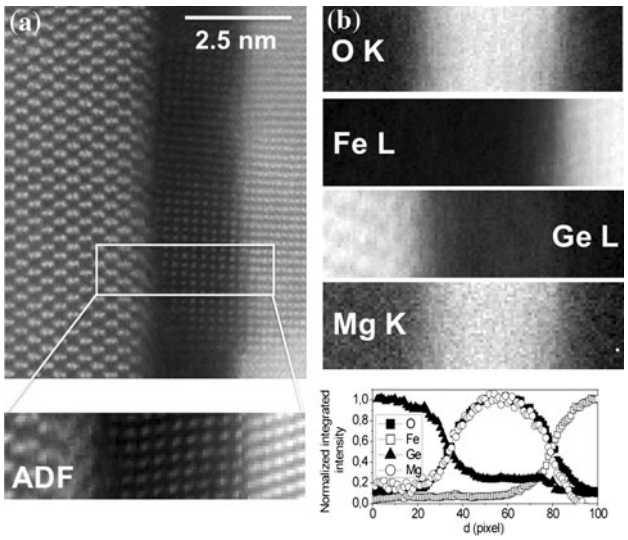

Fig. 3 Spectrum image of the epitaxial Fe/MgO/Ge(001) heterostructure obtained across the interfaces. **a** High resolution ADF image. A *square marks* the area where the spectrum image was acquired, containing the two interfaces, using a nominal acquisition time of 0.05 s per pixel. The *bottom panel* shows the ADF signal acquired simultaneously with the spectrum image. Minor spatial drift is present. **b** Chemical maps, after denoising with principal component analysis. From top to bottom: *O K* edge map, Fe $L_{2,3}$, Ge $L_{2,3}$ and Mg *K* maps. They all have been produced after background subtraction using apower law fit and integration of a 40 eV wide window. Since the Mg *K* edge sits on the tail of the Ge $L_{2,3}$ edge a second window for the power law fit was placed a few hundred eV after the edge onset. The *bottom panel* depicts the normalized integrated intensities along the growth direction for the four elemental maps, averaged over a window ten pixels wide in the direction parallel to the intefaces. Each pixel is equal to 0.4 Å

through a background subtraction and integration of the intensity remaining under every absorption edge [17]. This way, O, Fe, Ge, and Mg elemental maps were obtained, shown in Fig. 3b from top to bottom, respectively. The lowest panel of Fig. 3b shows the normalized integrated intensities averaged over a window ten pixels wide parallel to the interface direction for the four elemental maps. Within noise, the elemental signals fall from 75 to 25% intensity within one unit cell (roughly, half a nm) at both interfaces, which would be consistent with the interfaces being atomically sharp at least within the short lateral length scale (nanometric) probed by this data set. This is especially the case if one bears in mind that some electron beam broadening is present due to dechanneling through the sample thickness, which was estimated to be of 0.35 inelastic mean free paths from low loss measurements [18]. Even then, these results suggest that the Ge/MgO and the MgO/Fe interfaces are sharp, chemically speaking. Some residual intensity is measured within all the layers for some of the elements from the neighboring materials. This might be an artifact due to the presence of surface amorphous layers after the ion milling. On a longer lateral length scale, the interfaces are rough as shown by the z-contrast images. These undulations are, therefore, the result of physical roughness or step disorder present at the interfaces, and are mild enough that they do not seem to compromise the layers integrity, so no pinholes were observed.

Along with the chemical quantification, EEL spectroscopy allows extracting information about the electronic structure, such as the Fe–O bonding or the Fe oxidation state at different sites across the film. When Fe is oxidized to form a Fe–O compound, the fine structure of the *O K* edge exhibits a pre-peak feature at the *O K* onset [19]. Such feature can therefore be used to establish whether there is significant Fe oxidation through our Fe layers. Figure 4 summarizes the analysis of the fine structure of an EELS linescan across one of our Fe/MgO/(001)Ge heterostructures with the Au capping missing. Such linescans are recorded by acquiring EEL spectra while scanning the electron beam along a line such as the one marked on Fig. 4a. Figure 4b exhibits the EELS data for the whole linescan. Figure 4c shows average EELS spectra from different regions along the scan, after background subtraction using a power law. From bottom to top the spectra correspond to the Ge substrate, the Ge/MgO interface, the

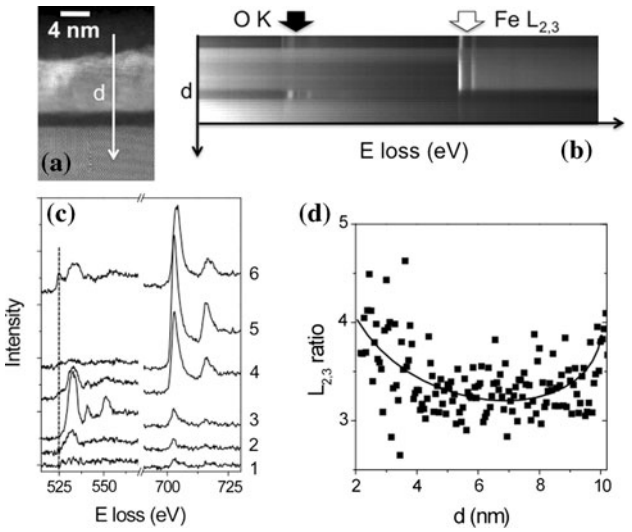

Fig. 4 **a** Low magnification ADF image of a Fe/MgO/Ge(001) heterostructure. The *white arrow* marks the region where an EELS linescan was acquired with an acquisition time of 0.5 s per pixel. **b** EELS linescan acquired along the *white arrow* in (**a**). The O *K* edges and Fe $L_{2,3}$ edges have been marked with *black* and *white arrows*, respectively. **c** Averaged EEL spectra resulting of adding five individual spectra along the linescan, displaced vertically for presentation purposes. The spectra correspond, from bottom to top, to: the Ge substrate (*1*), the Ge/MgO interface (*2*), the middle of the MgO layer (*3*), the MgO/Fe interface (*4*), the middle of the Fe layer (*5*) and the surface of the Fe layer (*6*). A *vertical dotted line* marks the O *K* pre-peak feature. **d** $L_{2,3}$ ratio within the Fe layer, along the direction marked with a *white arrow* in (**a**). The line is a guide to the eye

MgO layer, the MgO/Fe interface, the Fe layer and the surface of the Fe layer. Significant O is detected on the surface of the Fe layer for this uncapped portion of the sample, along with a significant *O K* pre-peak. These findings proof that the surface Fe is strongly oxidized, although it's worth mentioning that such Fe oxidation was not detected in EELS linescans from capped samples, where the Au protected the Fe layer. Interestingly, even in the case of lack of Au capping the O signal is practically zero in the middle of the Fe layer, as shown in Fig. 4c. At the Fe/MgO, the O signal increases due to the presence of the oxide. A very minor pre-peak is observed, pointing to a very low oxidation of Fe at this interface [20]. This finding is consistent with the high crystalline quality and the chemical sharpness reported above. No pre-peak is found within the insulating MgO layer.

The actual oxidation state of Fe can be quantified from the analysis of the fine structure of the Fe $L_{2,3}$ edge. For this aim, one of the most widely used methods is the calculation of the intensity ratio between the L_3 and L_2 peaks [19, 21–23], known as the $L_{2,3}$ ratio. The *L* edges in transition metals show two characteristic peaks, L_3 and L_2, that correspond to electron transitions from $2p_{3/2}$ and $2p_{1/2}$ core levels to unoccupied states in the 3*d* bands, respectively, as well as the continuum. The variation on the 3*d* occupancy then gets reflected in the intensity of the L_3 and L_2 peaks. The intensity ratio of the L_3 and L_2 lines of the Fe $L_{2,3}$ edge has been obtained here using the method described by Pearson/Egerton [17], which roughly means to remove the background below the Fe $L_{2,3}$ edge using a power fit and then remove the continuum contribution by scaling a step-function (e.g., a Hartree-Slater cross section function). For scaling purposes, it was used a 10 eV wide window placed right after the L_2 line as suggested in reference [24]. Next, the remaining signal under the thus corrected L_3 and L_2 lines was integrated within 10 eV wide windows. The resulting intensity values were then used to calculate the $L_{2,3}$ intensity ratio, $L_{2,3} = L_3/L_2$. Figure 4c shows the fine structure of the Fe $L_{2,3}$ from the Fe layer at different sites through the stacking, as described above. The $L_{2,3}$ ratio calculated from the EELS data is shown in Fig. 4d. The $L_{2,3}$ ratio has a value of 3.3 within the Fe layer, but increases to near 4.2 at the top surface. According to previous reports, the $L_{2,3}$ ratio increases with the oxidation of iron [19]. Also, a chemical shift of the Fe L_3 line a few eV towards higher energy is observed. Hence, the Fe atoms near the surface show a higher oxidation state, which is again consistent with the surface oxidation denoted by the O *K* edge. Again, this result is not surprising since no capping layer was present in this area of the sample to prevent the Fe layer from oxidation. A small increase of the $L_{2,3}$ ratio is also noticed within the last 0.5 nm (i.e., a unit cell or two) close to the Fe/MgO interface, but no noticeable chemical shift is observed. These facts are consistent with a minor oxidation of Fe, which is known to be critical to tunnel magnetoresistance properties [25]. Such oxidation is consistent with the very small O *K* pre-peak found, highlighting the high quality of the transition metal–oxide interface.

Summary

In summary, the authors have shown that Z-contrast and EELS imaging in the aberration corrected STEM provide both a qualitative and also a quantitative characterization of epitaxial Fe/MgO/(001)Ge heterostructures of interest for applications in electronics and spintronics. ADF images show that the layers in these heterostructures are relatively flat and continuous over long lateral distances. The interfaces show some roughness in the form of steps, but they don't compromise the integrity or morphology of the layers. Interfacial defects such as mismatch dislocations are observed. The interfaces are not perfectly coherent, but the epitaxial relationship is preserved from layer to layer and the overall crystal quality is good. Atomic resolution EEL spectrum imaging allows the acquisition of elemental maps

for O, Fe, Ge and Mg, all the elements of interest in this system. These elemental maps are consistent with chemically sharp interfaces with no major chemical intermixing and no secondary oxide phases formation at the Fe/MgO interfaces. These results show that the epitaxial growth of good quality Fe/MgO/(001)Ge heterostructures suitable for tunneling contacts between a ferromagnet and a semiconductor is, indeed, possible.

Acknowledgements This study supported by the European Research Council Starting Investigator Award (JG), the U.S. Department of Energy, Office of Basic Energy Sciences, Materials Sciences and Engineering Division (MV) and by the Fondazione Cariplo via project MANDIS (Project no. 2007.5095) (D.P., M. C, C. R., S. B., and R. B.). The authors are thankful to J.T. Luck for STEM specimen preparation and to M. Watanabe for the plug in for Principal Component Analysis into Digital Micrograph.

References

1. Zhou Y, Ogawa M, Han X, Wang KL (2008) Alleviation of fermi-level pinning effect on metal/germanium interface by insertion of an ultrathin aluminum oxide. Appl Phys Lett 93:202105
2. Zhou Y, Ogawa M, Bao M, Wei H, Kawakami RK, Wang KL (2009) Engineering of tunnel junctions for prospective spin injection in germanium. Appl Phys Lett 94:242104
3. Martinez Boubeta C, Navarro E, Cebollada A, Briones F, Peiro F, Cornet A (2001) Epitaxial Fe/MgO heterostructures on GaAs (001). J Cryst Growth 226:223
4. Butler WH, Zhang XG, Schuthess TC, MacLaren JM (2001) Spin-dependent tunneling conductance of Fe|MgO|Fe sandwiches. Phys Rev B 63:054416
5. Ganichev SD, Danilov SN, Bel'kov VV, Giglberger S, Tarasenko SA, Ivchenko EL, Weiss D, Jantsch W, Schäffler F, Gruber D, Prettl W (2007) Pure spin currents induced by spin-dependent scattering processes in SiGe quantum well structures. Phys Rev B 75:155317
6. Browning ND, Chisholm MF, Pennycook SJ (1993) Atomic-resolution chemical analysis using a scanning transmission electron microscope. Nature 366:143
7. Nellist PD, Pennycook SJ (1998) Subangstrom resolution by underfocussed incoherent transmission electron microscopy. Phys Rev Lett 81:4156
8. Nellist PD, Chisholm MF, Dellby N, Krivanek OL, Murfitt MF, Szilagyi ZS, Lupini AR, Borisevich AY, Sides WH, Pennycook SJ (2004) Direct sub-angstrom imaging of a crystal lattice. Science 305:1741
9. Jia CL, Lentzen M, Urban K (2004) High-resolution transmission electron microscopy using negative spherical aberration. Microsc Microanal 10:174
10. Bosman M, Keast VJ, Garcia-Muñoz JL, D'Alfonso AJ, Findlay SD, Allen LJ (2007) Two-dimensional mapping of chemical information at atomic resolution. Phys Rev Lett 99:086102
11. Kimoto K, Asaka T, Nagai T, Saito M, Matsui Y, Ishizuka K (2007) Element-selective imaging of atomic columns in a crystal using STEM and EELS. Nature 450:702
12. Varela M, Findlay SD, Lupini AR, Christen HM, Borisevich AY, Dellby N, Krivanek OL, Nellist PD, Oxley MP, Allen LJ, Pennycook SJ (2004) Spectroscopic imaging of single atoms within a bulk solid. Phys Rev Lett 92:095502
13. Varela M, Lupini AR, Benthem K, Borisevich AY, Chisholm MF, Shibata N, Abe E, Pennycook SJ (2005) Materials characterization in the aberration-corrected scanning transmission electron microscope. Ann Rev Mater Res 35:539
14. Petti D, Cantini M, Rinaldi C, Brivio S, Bertacco R, Gazquez J, Varela M (2010) Sharp Fe/MgO/Ge(001) epitaxial heterostructures for tunneling junctions. (in preparation)
15. Vassent JL, Dynna M, Marty A, Gilles B, Patrat G (1996) A study of growth and the relaxation of elastic strain in MgO on Fe(001). J Appl Phys 80(10):5727
16. Muller DA, Fitting-Kourkoutis L, Murfitt M, Song JH, Wang HY, Silcox J, Dellby N, Krivanek OL (2008) Atomic-scale chemical imaging of composition and bonding by aberration-corrected microscopy. Science 319:1073
17. Egerton RF (1996) Electron energy loss in the electron microscope, 2nd edn. Plenum, New York
18. Oxley MP, Varela M, Pennycook TJ, van Benthem K, Findlay SD, D'Alfonso AJ, Allen LJ, Pennycook SJ (2007) Interpreting atomic-resolution spectroscopic images. Phys Rev B 76:064303
19. Colliex C, Manoubi T, Ortiz C (1991) Electron-energy-loss-spectroscopy near-edge fine structures in the iron-oxygen system. Phys Rev B 44:11402
20. Serin V, Andrieu S, Serra R, Bonnel F, Tiusan C, Calmels L, Varela M, Pennycook SJ, Snoeck E, Walls M, Colliex C (2009) TEM and EELS measurements of interface roughness in epitaxial Fe/MgO/Fe magnetic tunnel junctions. Phys Rev B 79:144413
21. Kurata H, Colliex C (1993) Electron-energy-loss core-edge structures in manganese oxides. Phys Rev B 48:2102
22. Riedl T, Gemming T, Runner W, Acker J, Wetzig K (2007) Determination of manganese valency in $La_{1-x}Sr_xMnO_3$ using ELNES in the (S)TEM. Micron 38:224
23. Waddington WG, Rez P, Grant IP, Humphreys CJ (1986) White lines in the L2, 3 electron-energy-loss and X-ray absorption spectra of 3d transition metals. Phys Rev B 34:1467
24. Varela M, Oxley MP, Luo W, Tao J, Watanabe M, Lupini AR, Pantelides ST, Pennycok SJ (2009) Atomic-resolution imaging of oxidation states in manganites. Phys Rev B 79:085117
25. Miyokawa K, Saito S, Katayama T, Saito T, Kamino T, Hanashima K, Suzuki Y, Mamiya K, Koide T, Yuasa S (2005) X-ray absorption and X-ray magnetic circular dichroism studies of a monatomic Fe(001) layer facing a single-crystalline MgO(001) tunnel barrier. Jpn J Appl Phys Part 2 44:L9